2020 17TH INTERNATIONAL CONFERENCE ON ELECTRICAL ENGINEERING, COMPUTING SCIENCE AND AUTOMATIC CONTROL (CCE)
MEXICO CITY, MEXICO. NOVEMBER 11-13, 2020

Spiking Neural Network Architecture Comparison by Solving the Non-linear XOR Problem

A. Anzueto-Ríos, F. Gómez-Castañeda, and J.A. Moreno-Cadenas
Electrical Engineering Department, Cinvestav-IPN, Mexico City, Mexico
phone no. (+52) 55 5747 3800 Ext. 6261
e-mail:{alvaro.anzueto, fgomez, jmoreno}@cinvestav.mx

***Abstract*—This work presents an analog model for a cellular membrane of a neuron as well as its mathematical analysis. The simple model of a spiking neuron from Izhikevich is used to design two neural architectures. From the electrical analysis the synaptic current is obtained and used as an input parameter to the Izhikevich's model. The first architecture has two neurons on the input layer and one on the output layer, using this architecture it is shown that the neuron models based on the behavior of biologic neurons can be used in a similar manner to the well-known second generation neural networks to solve classification problems. Moreover, in the present work it is shown the superiority of the spiking neuron models, which leads to the second architecture to be conformed by a single neuron. Both architectures are compared performance wise, through the classic problem of separating a non-linear dataset, XOR. The results show that these architectures can be used to the classification or clustering of patterns of features.**

***Index Terms*—Izhikevich neuron model, spiking neural network, membrane mathematical model, neural architecture, XOR problem, metaheuristics, EABC algorithm.**

I. Introduction

The artificial neural network models have always had the objective of approaching the behavior of biological neurons, thus simple models have been produced to describe such functioning, these models try to emulate the communication process through synapses and the synaptic plasticity by which the existing relations are modified. From [1], [2], neural networks can be classified in 3 generations. The first generation of neural networks are those that follow the neuron model proposed by McCulloch-Pitts [3] which is based on a simple processing unit known as perceptron. These neurons are activated when a threshold value is surpassed and, one characteristic of this model is that the output is either 0 or 1. The second generation of neural networks consists of two computation units, namely one which sums the synaptic inputs and the second one which is represented by an activation function and generates the output. The activation functions can be linear, sigmoidal, hyperbolic or any other that defines a range of values as output. The third generation of neural networks approaches better the behavior of biological neural networks most of the time. These networks occupy models to reproduce the train pulses commonly present in the biological networks to communicate them. Many studies of these networks appeared in the last years given the accumulated evidence that pointed to the fact that biological neurons use dynamic membrane potentials, also known as spikes, to encode and process information. The XOR problem, is widely used because it is an example of a non-linear separable problem [4], [5]. Some solutions propose using spiking neural networks (SNN). Comsa M. et. al [5] proposed an SNN architecture based on the membrane cellular model known as Spike Response Model (SRM), [6]. The SRM model is a simplified model proposed by Hodgkin-Huxley, which considers the membrane potential. This work shares a similar idea to perform the electrical analysis of the membrane potential and its behavior is described mathematically. The SRM model can be considered not so practical due to its bad behavior when the threshold value is surpassed. When this happens, the neuron enters into a standby state that does not produce an output spike as expected, that is why for this work the model proposed by Izhikevich [7], [8] is considered.

In this work, the Efficient Artificial Bee Colony or EABC metaheuristic optimization method has been used to compute the synaptic weights of the proposed architectures. In [9], it is shown the excellent performance of the EABC in finding the solution parameters with and without restrictions. This favors its application in this work.

This model approximates better the biologic behavior and it is computationally less complex. As a consequence of trying to demonstrate the superior capacity of the biological neural models it is shown that a single spiking neuron can solve complex problems and grouped can be used to solve data separation problems.

II. Methodology

A. Electrical model of the cellular membrane

This section will explore the biophysical mechanism behind the generation of neural activity. Thus, the biological and electrical representation will be described. Fig.1 shows an electrical diagram which is an analog representation of the components on a neuron [10]. The positive and negative signs, surrounding the membrane represent charges inside and outside it. Moreover, both the electrical resistance and capacitance associated to the membrane are represented too. Finally, the external current contribution is also represented through the electrode I_e.

The total capacitance and resistance of the membrane are represented by C_m and R_m, respectively. The membrane capacitance is represented as c_m and a typical value is $c_m \approx 10\,{}^{nF}\!/_{mm^2}$. So, to calculate C_m the below equation is used.

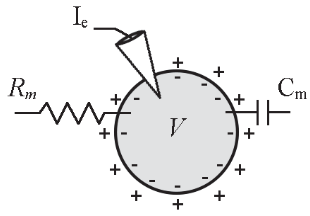

Fig 1. Analogous representation of a neuron cell. Based on [10]

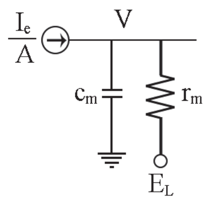

Fig 2. RC circuit equivalent to the neuron membrane. Based on [10]

$$C_m = c_m A \tag{1}$$

In a similar manner $r_m \approx 1\,M\Omega{\cdot}mm^2$. The total resistance of the membrane is calculated using (2).

$$R_m = {}^{r_m}\!/_{A} \tag{2}$$

In Fig.1 I_e is a small current which is injected using an electrode. If Ohm's law is applied, $\Delta V = I_e R_m$ then the electric neuronal activity is obtained only if the injected current is applied at regular time intervals. When this current is stopped then the cell will reach a relaxing state also known as equilibrium state. In this way, the membrane current can be known. This current is determined in its totality by the opening and closing of the sodium and potassium ionic channels. The total current on the membrane is determined by the sum of currents. They are due to the difference between opening and closing ionic channels, and this phenomenon leads also to a synaptic potential.

The total current present on the membrane is obtained multiplying i_m by the cell's surface, this can be appreciated with (3).

$$I_m = i_m A \tag{3}$$

Hodgkin and Huxley presented a model that mainly considers sodium and potassium ions, but they expressed the possibility of existence of other ion types [11]. In (4), g_i is the specific conductance due to the ionic channels and E_i is the equilibrium potentials associated with the ion channels that are considered.

$$i_m = \sum_i g_i \left(V - E_i\right) \tag{4}$$

In Fig.2. a RC model electrically equivalent to the membrane is presented. Where c_m and r_m represent the capacitance and resistance of the membrane respectively, E_L denotes the equilibrium potential of the neuron and I_e is an external injected current. Table I shows the typical values considered for this model.

Table I
MEMBRANE PARAMETERS

Parameter	Typical value
c_m	$\approx 10^{nF}/_{mm^2}$
r_m	$\approx 1M\Omega \cdot mm^2$
C_m	$c_m A$
R_m	${}^{r_m}/_{A}$
E_L	$-70mV$

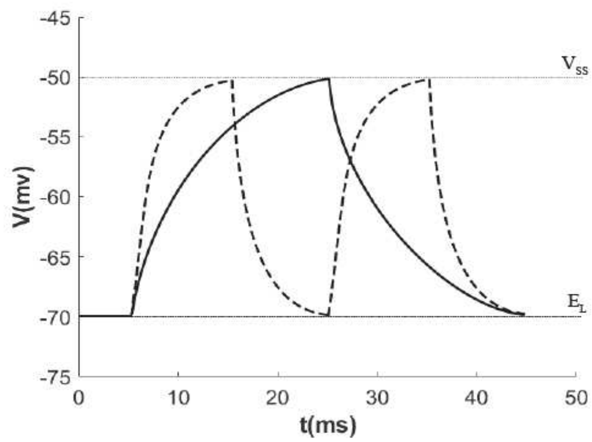

Fig 3. Membrane potential. Dashed line: τ_m=10ms, solid line: τ_m=20ms. For both graph $V_{ss} = 50mV$ and $E_L = -70mV$.

For the proposed RC circuit, we should consider its behavior through time generating (5), (6) and (7). With these equations it is possible to obtain the value of the current which is time dependent. Considering (6) the right-hand expression is obtained using the Kirchhoff-law of currents sum. The negative sign on the first factor points to an inverse current with respect to the analysis of node V. The left part represents the current derived from the variation of the membrane capacitance through time.

$$i = C_m \frac{dv}{dt} \tag{5}$$

$$c_m \frac{dV}{dt} = -\frac{(V - E_L)}{r_m} + \frac{I_e}{A} \tag{6}$$

$$\tau_m \frac{dV}{dt} = -\left(V - E_L\right) + I_e R_m \tag{7}$$

In (7), we multiply r_m on both sides of (6) we would have $\tau_m = r_m c_m = R_m C_m$, which τ_m is the time constant of the membrane and plays an important role determining how fast a neuron cell reacts on changes to the input. Therefore, a big τ_m implies a slow response and a small τ_m represents a fast response of the neuron, refer to plot in Fig. 3 V_{ss} is the value of the neuron in a stable state with an input current and is calculated using (8). When the external current stops flowing the potential decreases to its equilibrium state E_L.

$$V_{ss} = E_L + I_e R_m \tag{8}$$

Until this point it has only considered the behavior of the cellular membrane, however, for this work it is important to analyze the presence of a synaptic potential and how this modifies the cellular behavior, therefore the behavior shown

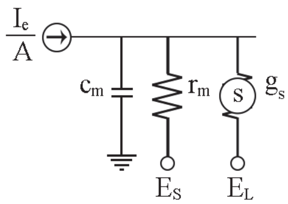

Fig 4. Equivalent RC circuit with synaptic conductance. Base on [10]

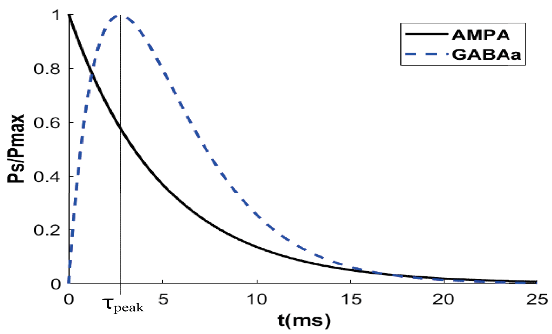

Fig 5. Synaptic response AMPA & GABA$_A$

on the RC model will be enriched with the presence of the synapses. The synaptic presence modelled as a conductance is expressed by (9) and presented on Fig. 4

$$\tau_m \frac{dV}{dt} = -\left(\left(V - E_L\right) + g_s\left(V - E_s\right) r_m\right) + I_e R_m \tag{9}$$

In (9), it is important to determine the value of the synaptic conductance considering the opening of the ionic channels; for this condition it will be considered the probability of the channels being opened or closed at a certain point in time. With that in mind, expression (10) is obtained, $g_{s,max}$ represents la conductance associated to the synapses, P_{rel}, is the probability of generating an output spike due to the presence of an input spike and P_s is the probability of opening of the postsynaptic ionic channels. The relation between P_s and P_{rel} can be seen on the Fig. 5. In that figure the behavior of two receptor types of chemical synapses through time ($AMPA, GABA_A$) can be appreciated. Equation (11) expresses the form of the $AMPA$ (a-amino-3-hydroxy-5-methyl-4-isoxazolepropionic acid receptor) synapses and (12) does the same with the $GABA_A$ (gamma-aminobutyric acid receptor) synapses. τ_{peak} is the time that elapses after a pulse has been given at the input and the maximum value of the function (12) is reached. In Fig. 3 $\tau_{peak} = 2.7ms$.

$$g_s = g_{s,max} P_{rel} P_s \tag{10}$$

$$K\left(t\right) = e^{-\frac{t}{\tau_s}} \tag{11}$$

$$\alpha\left(t\right) = \frac{t}{\tau_{peak}} \cdot e^{\left(1 - \frac{t}{\tau_{peak}}\right)} \tag{12}$$

Previous equations have considered the presence of a single spike, however, a closest approach to the biological behavior should consider the presence of spike trains at the input. Concerning the presence of multiple spikes (See Fig 6.), leads to equation (13) from which the set of discrete values t_i are

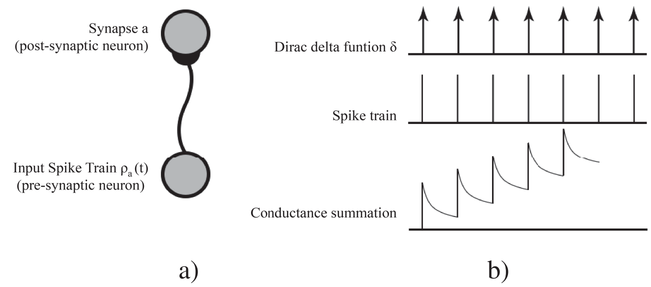

Fig 6. a) Pre-synaptic and post-synaptic neuron. b) Over time representation of the conductance variance.

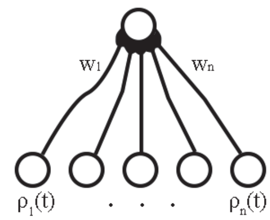

Fig 7. Neuron with multiple synapses input.

the points in time associated to spikes presence. δ is the Dirac function which means that only the spike's generation time is taken into account.

$$\rho_a\left(t\right) = \sum_i \delta\left(t - t_i\right) \tag{13}$$

The synaptic conductance at the input of a neuron is calculated using (14). This equation models how synaptic conductance changes on the post-synaptic neuron. Basically, it represents the sum of all the multiple functions (11) or (12), associated with spikes present in the pre-synaptic neuron.

A representation of how an input spike train modifies the conductance g_a through time, is presented on Fig 6. b)

$$g_a\left(t\right) = g_{a,max} \int_{-\infty}^{t} K\left(t - \tau\right) \rho_a\left(\tau\right) d\tau \tag{14}$$

Now, considering that a neuron can have connections to multiple synapses, this is represented in Fig. 7

For this case the total synaptic current of a neuron is calculated by the expression in (15), in which it is performed the summation of the synaptic contribution, where the subindex b represents specific synapses connected to the neuron. Using (14), the total dynamic synaptic current on the neuron is expressed by (16). Where the parameter w represents the synaptic weight. Equation (17) approaches (16), where $\left(u_b\left(\tau\right)\right)$ takes into account the discrete values in time of the instantaneous spikes.

$$I_s\left(t\right) = \sum_{b=1}^{N} I_b\left(t\right) \tag{15}$$

$$I_s\left(t\right) = \sum_{b=1}^{N} w_b \int_{-\infty}^{t} K\left(t - \tau\right) \rho_b\left(\tau\right) d\tau \tag{16}$$

$$I_s(t) \approx \sum_{b=1}^{N} w_b \int_{-\infty}^{t} K(t-\tau)\, u_b(\tau)\, d\tau \tag{17}$$

Equation (17) leads to (18), where $K(t) = \frac{1}{\tau_s} e^{-\frac{t}{\tau_s}}$ and τ_s represents the neuron change rate when is in the presence of the input currents of each synapses. Equation (19) represents the complementary variable in this systems namely, the spike voltages; where the function $F(.)$ relates current and voltage. An alternative manner to represent (18) is using (20), where the synaptic weights are contained by the matrix $\mathbf{W}$ and the input current by the vector $\mathbf{u}$. Finally, the equations (21) and (22) formulate the steady state of the spiking neurons.

$$\tau_s \frac{dI_s}{dt} = -I_s + \sum_b w_b u_b \tag{18}$$

$$\tau_r \frac{dv}{dt} = -v + F(I_s(t)) \tag{19}$$

$$\tau_s \frac{dI_s}{dt} = -I_s + \mathbf{W} \cdot \mathbf{u} \tag{20}$$

$$0 = -I_s + \mathbf{W} \cdot \mathbf{u} \tag{21}$$

$$V = F(\mathbf{W} \cdot \mathbf{u}) \tag{22}$$

B. Izhikevich Neuron Model

Izhikevich [7], [8] proposes a neural model that reproduces the spikes of cortical neurons. This model combines the biological plausibility of the Hodgkin-Huxley model and the computational efficiency from the integrate and fire model. The equations of this model are expressed on (23), (24) and (25).

$$C \frac{dv}{dt} = k(v - v_r)(v - v_t) - u + I \tag{23}$$

$$\frac{du}{dt} = a(b(v - v_r) - u) \tag{24}$$

$$\text{if } v \geq v_{peak} \Rightarrow v = c,\ u = u + d \tag{25}$$

The parameters in Table II are the following: v is the membrane voltage, u is the recovery current, C is the membrane capacitance, v_r sis the resting membrane potential and v_t, is the instantaneous threshold potential. The constant a is the recovery time and, the sign of b, which is another constant, determines if u is an amplifying or resonant variable. The constant c describes the after-spike reset value of the membrane potential v caused by the fast high-threshold K^+conductances, and d describes after-spike reset of the recovery variable u caused by slow high-threshold $Na^+$and K^+ conductances [7], [8].

The neural model can be modified based on four parameters achieving different configurations on the pulse generation response. In Fig. 8, it is presented the different choices of parameters on each configuration. The present work reproduces the behavior of a "regular spiking" (RS) configuration (see Table II).

The parameter I in (23), is obtained from (21) considering the input values and their corresponding synaptic weights.

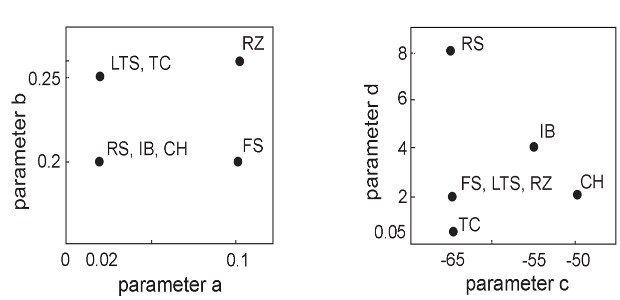

Fig 8. Selection value of parameters from Izhikevich model. From [7]

Table II
PARAMETER VALUES OF IZHIKEVICH'S MODEL

Parameter	Value
a	0.03
b	-2
c	-50
d	100
v_r	-60
v_t	-40
C	100
k	0.7
v_{peak}	35

Morales de-la-Rosa [12] observes that the Izhikevich model can generate pulses with current values above $50pA$.

C. Feedforward Neural Network

With the previous definitions it can be modelled feedforward neural networks, like those in Fig. 9 Where S_y represents the synaptic input. In the Izhikevich neuron model and w the synaptic weights. In Fig. 9b), it is presented an architecture traditionally used by the second generation neural networks with the purpose of showing that it is possible to have a similar architecture with third generation neural networks, achieving the solution of non-linear problems, like the XOR problem. However, the models based on the third generation, have shown to be robust compared to the second-generation; the present work shows this by solving the XOR problem using a single neuron. Based on (22) two functions have been considered to obtain the membrane voltage. One function with radial basis functions (26) applied to the architecture on Fig. 8b) and a second polynomial function, presented in (27), applied to the architecture on Fig. 8a.

$$I = e^{\frac{-\parallel x - w' \parallel^2}{2\sigma 2}} + \eta \tag{26}$$

$$I = (x \cdot w' + 1)^p + \eta \tag{27}$$

In (26) and (27), η is an offset current for supporting the generation of spikes. Its value in the next experiments was $55pA$.

Using the results developed so far, a feedforward neural architecture can be implemented to classify patterns.

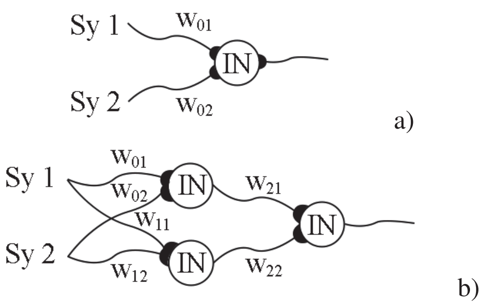

Fig 9. Feedforward neural architecture. a)Architecture "A", b)Architecture "B"

Table III
ARCHITECTURES RESPONSE.

S_Y1	S_Y2	Arc. "A"	Arc. "B"
0	0	3 spike	2 spike
0	1	2 spike	3 spike
1	0	2 spike	3 spike
1	1	3 spike	2 spike

III. RESULTS

A representative spiking response of the architectures "A" using Izhikevich neuron model is shown in Fig.10. The synaptic input values S_y1, S_y2 and its output the number of pulses generated by the output neuron are presented in Table III.

In Fig.11, it is shown a 3D plot of the behavior of the neural architecture when its values on the synaptic inputs are varied. For this graph, the X axis corresponds to the synaptic input S_y1 and the Y axis to the input S_y2. The Z axis is the number of generated pulses at the output of the architecture. In Fig.11a) it is shown the isometric view and Fig.11b) is the upper view of the neural architecture "A" output response. It is important to note that in this architecture a polynomial function (27), has been applied as activation function; therefore, the transition from one type of response to the other is determined by a straight line.

Fig.12 and Fig.13 show the results obtained when the neural architecture "B" is considered. In this scenario, the radial basis function (26) is used. It is important to note that the transition between responses correspond to a radial basis function.

The values for the weight matrix **W** in (21), has been calculated using the metaheuristic optimization EABC algorithm [9] and results obtained for both neural architectures are shown on Table IV. The values for the synaptic weights have been calculated using the mean value over 100 executions of the ABC algoritm. These results express the feasibility of the presented architectures.

IV. CONCLUSION.

In this work, an electrical model of the neuronal cell membrane was presented, and a mathematical analysis was performed to determine the synaptic current at the input. The calculated synaptic current was used as an input parameter on the Izhikevich neuron model. Two architectures were shown, both of them are able to solve a non-linear separation problem (XOR). The first neural architecture "A"

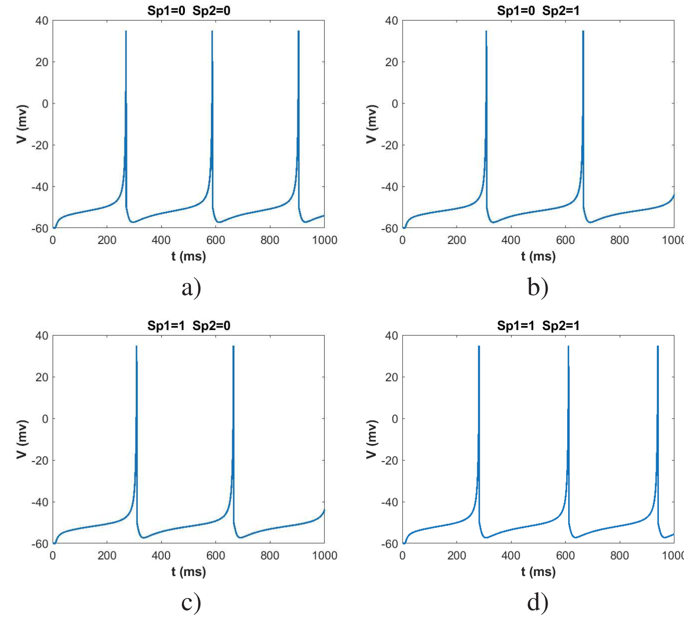

Fig 10. Architecture "A" response with synaptic input.

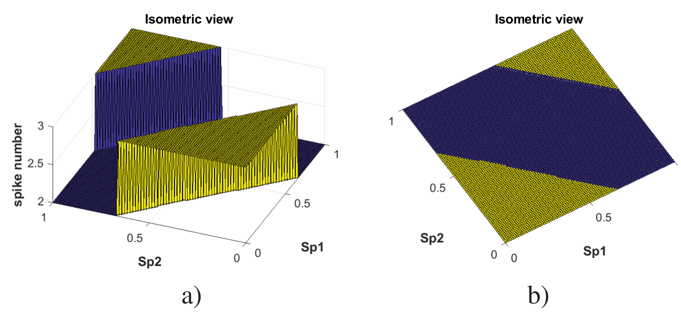

Fig 11. Architecture "A" response 3D graphics. a) Isometric view, b) Upper view

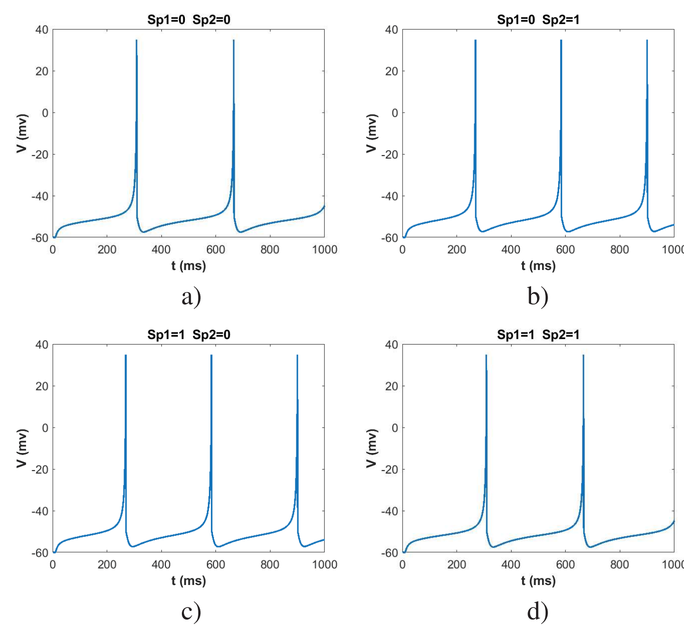

Fig 12. Architecture "B" response with synaptic input.

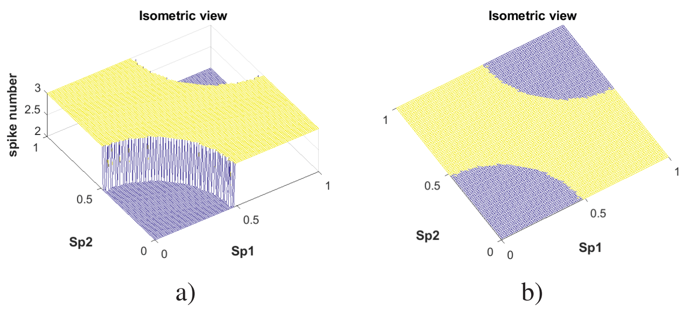

Fig 13. Architecture “B” response 3D graphics. a) Isometric view, b) Upper view

Table IV
SYNAPTIC WEIGHTS CALCULATED USING EABC ALGORITHM.

Efficient ABC algorithm	
Parameter	Value
N	100
L	100
Max. Iter.	1000
u_i	0
l_i	100
Architecture “A”	
w_{01}	-0.9001
w_{10}	-0.9002
Architecture “B”	
w_{01}	0.0012
w_{02}	0.0009
w_{11}	0.9996
w_{12}	0.9991
w_{21}	1.9992
w_{22}	1.9995

shows that third generation neurons have similar capabilities with second generation architectures. The second neuronal architecture B, is comparable with the biological neurons, due to its ability to solve non-linear separability problems. Thus, this work shows that these type of neurons can be used to solve clustering problems on patterns of features with static inputs. The numeric results obtained express the feasibility of more architectures different from those presented in this work, and open the possibility to work with more complex datasets.

REFERENCES

[1] S. Davies, *Learning in spiking neural networks*. PhD thesis, Citeseer, 2013.

[2] W. Maass, “Networks of spiking neurons: the third generation of neural network models,” *Neural networks*, vol. 10, no. 9, pp. 1659–1671, 1997.

[3] W. S. McCulloch and W. Pitts, “A logical calculus of the ideas immanent in nervous activity,” *The bulletin of mathematical biophysics*, vol. 5, no. 4, pp. 115–133, 1943.

[4] D. Huderek, S. Szczęsny, and R. Rato, “Spiking neural network based on cusp catastrophe theory,” *Foundations of Computing and Decision Sciences*, vol. 44, no. 3, pp. 273–284, 2019.

[5] I. M. Comsa, T. Fischbacher, K. Potempa, A. Gesmundo, L. Versari, and J. Alakuijala, “Temporal coding in spiking neural networks with alpha synaptic function,” in *ICASSP 2020-2020 IEEE International Conference on Acoustics, Speech and Signal Processing (ICASSP)*, pp. 8529–8533, IEEE, 2020.

[6] W. Gerstner, “A framework for spiking neuron models-the spike response model,” *Handbook of Biological Physics*, vol. 4, no. BOOK_CHAP, pp. 469–516, 2001.

[7] E. M. Izhikevich, “Simple model of spiking neurons,” *IEEE Transactions on neural networks*, vol. 14, no. 6, pp. 1569–1572, 2003.

[8] E. M. Izhikevich, *Dynamical systems in neuroscience*. MIT press, 2007.

[9] J. Enríquez-Gaytán, F. Gomez-Castañeda, J. A. Moreno-Cadenas, and L. M. Flores-Nava, “Experimental spiking neural network: Solving the xor paradigm with metaheuristics,” in *2018 15th International Conference on Electrical Engineering, Computing Science and Automatic Control (CCE)*, pp. 1–5, IEEE, 2018.

[10] P. Dayan and L. F. Abbott, “Theoretical neuroscience: computational and mathematical modeling of neural systems,” 2001.

[11] A. L. Hodgkin and A. F. Huxley, “A quantitative description of membrane current and its application to conduction and excitation in nerve,” *The Journal of physiology*, vol. 117, no. 4, p. 500, 1952.

[12] E. Morales-DelaRosa, “Prototipo en fpga de emulador de red neuronal pulsada,” Master’s thesis, Cinvestav, 2019.